Molecular Crystals and Liquid Crystals

ISSN: 1542-1406 (Print) 1563-5287 (Online) Journal homepage: https://www.tandfonline.com/loi/gmcl20

Double resonance raman spectrain disordered graphite and singlewall carbon nanotubes

R. Saito , A. Grueneis , L. G. Cancado , M. A. Pimenta , A. Jorio , G. Dresselhaus , M. S. Dresselhaus & A. G. Souza Filho

To cite this article: R. Saito , A. Grueneis , L. G. Cancado , M. A. Pimenta , A. Jorio , G. Dresselhaus , M. S. Dresselhaus & A. G. Souza Filho (2002) Double resonance raman spectrain disordered graphite and singlewall carbon nanotubes, Molecular Crystals and Liquid Crystals, 387:1, 63-72, DOI: 10.1080/10587250215240

To link to this article: https://doi.org/10.1080/10587250215240

Mol. Cryst. Liq. Cryst., Vol. 387, pp. [287]/63–[296]/72

1058-725X/02 $12.00 + .00
DOI: 10.1080/10587250290113565

DOUBLE RESONANCE RAMAN SPECTRA IN DISORDERED GRAPHITE AND SINGLE WALL CARBON NANOTUBES

R. Saito and A. Grueneis
Dept. of Electronic Engineering, Univ. of Electro-Communications, Chofu, 182-8585 Tokyo, Japan

L. G. Cancado and M. A. Pimenta
Dept. de Física, Univ. Federal de Minas Gerais, Belo Horizonte - MG, 30123-970 Brazil

A. Jorio
Dept. of Physics

G. Dresselhaus
Francis Bitter Magnet Laboratory

M. S. Dresselhaus
Dept. of Physics; Dept. of Electrical Engineering and Computer Science, Massachusetts Institute of Technology, Cambridge, MA 02139-4307, USA

A. G. Souza Filho
Dept. de Física, Univ. Federal do Ceará, Fortaleza-CE, 60455-760 Brazil

The Raman spectra of the disorder-induced D-band and some other non-zone-center phonon modes of graphite and single wall carbon nanotubes are discussed using double resonance Raman theory. For two-dimensional disordered graphite, two D-band peaks and one G′-band peak are predicted. The trigonal

The authors thank many collaborators for doing the experiments related to this subject. R.S. acknowledges UFMG for supporting the visit to UFMG on this subject and a Grant-in-Aid (No. 13440091) from the Ministry of Education, Science, Japan. M.A.F. acknowledges NSF-CNPq joint collaboration grant (CNPq #910120/99-4). A.J./A.G.S.F. acknowledge support from the Brazilian agencies CNPq/CAPES. The MIT authors acknowledge support under NSF Grants DMR 01-16042, INT 98-15744, and INT 00-00408.

warping effect of the constant energy contours in graphite and the van Hove singularities in the electronic and phonon energy dispersion of carbon nanotubes are of importance for discussing the line width and possible numbers of Raman peaks which come from inequivalent Raman processes.

Keywords: carbon nanotubes; Raman spectroscopy; D-band; double resonance; dispersive phonon modes

INTRODUCTION

Recently, the disorder-induced Raman peak (D-band) observed around $1350\,\mathrm{cm}^{-1}$ for laser excitation energy $E_{\mathrm{laser}} = 2.41$ eV [1–5] and other weak phonon modes appearing in the intermediate frequency region [6] are discussed using the double resonance Raman theory for graphite and for single wall carbon nanotubes(SWNTs). In the double resonance Raman theory, the origin of the D-band and of the many unassigned phonon peaks in the Raman spectra is explained by (1) a second-order scattering process and (2) resonant enhancements of the Raman intensity in the two consecutive scattering processes. In the second-order scattering process, an electron with momentum k is: (a) at first excited by the incident photon, (b) scattered to state $k + q$ and (c) then back-scattered to state k and finally (d) recombined with a hole to yield the scattered photon [see Fig. 1(b)]. If two of the three intermediate states from (a) to (c) correspond to real electronic states in the energy dispersion, $E(k)$ and $E(k + q)$, the Raman intensity is enhanced by two resonant factors among the three energy difference denominators occurring in the intensity formula, and this is known as the double resonance Raman process [7]. Since one of two scattering processes is an inelastic phonon emission (or absorption), another scattering process that occurs is not phonon-related, but is instead due to impurity scattering induced by a defect or an edge of the graphitic material. Most impurity scattering is known to be energy conserving, elastic scattering, which we will consider here. In general, double resonance processes in a semiconductor are considered to be scattering within a single energy surface [7]. However, in graphite, the double resonance process over inequivalent Fermi surfaces (inter-valley scattering) is possible, too. The inter-valley scattering has a large phonon q vector which is relevant to the D-band frequency [4–6]. Here we consider detailed aspects of the second-order, one-phonon, and inter-valley Raman scattering process in two (three) dimensional (2D, 3D) graphite and in a SWNT, using double resonance theory.

In the double resonance Raman process, the intermediate $E(k + q)$ states are always real electronic states and another resonance condition is satisfied by resonance of an electronic state with either the incident or the

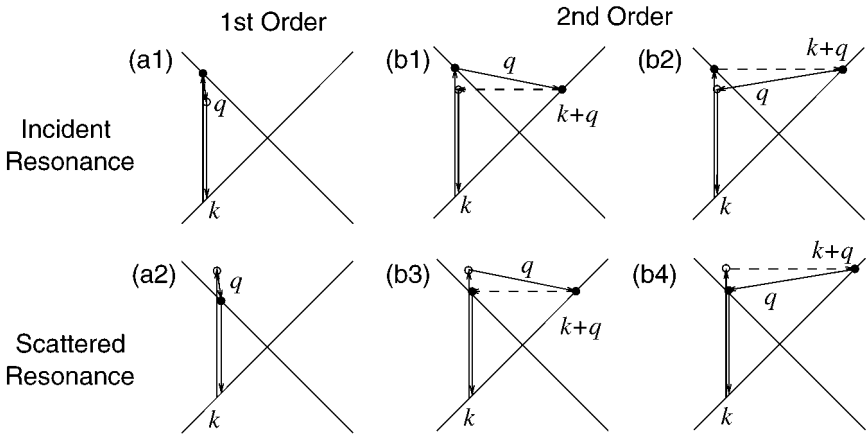

FIGURE 1 (a) First-order Raman processes which are resonant with (a1) the incident and (a2) the scattered laser light. Solid and open dots denote resonance and non-resonance scattering, respectively. Crossed lines show the linear energy dispersion of 2D graphite around the K point. (b) Second-order Raman processes which are resonant with (b1,b2) the incident and (b3,b4) the scattered laser light. The solid scattered vectors and dashed scattered vectors with wavevector q, respectively, denote inelastic and elastic scattering processes.

scattered laser photons. Resonance with the incident or scattered photon also exists in the first-order resonant Raman process [see Fig. 1(a)], in which the phonon wave vector q is small since the photon wave vector is small to make a vertical transition. This is the reason why we generally observe zone center phonon modes ($q = 0$) in first-order Raman spectroscopy. In second-order processes, however, since energy and momentum conservation is required for each process, $E(k+q) = E(k) - \hbar\omega(q)$ is satisfied for electronic and phonon energy dispersions, $E(k)$ and $\hbar\omega(q)$, respectively, where the phonon wave vector can be taken arbitrarily. Thus, the double resonance Raman peak is not limited to zone-center phonon modes. In the case of graphite, since there are two distinct k regions [for energy contours $E = E(k)$] around the K and K′ points [see Fig. 2(a)], which are inequivalent corners in the hexagonal Brillouin zone (BZ), the phonon wave vectors q can be considered for two cases; one is for scattering within the same region around the K (or K′) point (q_{intra}), and the other is for scattering from K to K′ (or K′ to K) (q_{inter}), which we call, respectively, intra-valley and inter-valley scattering [Fig. 2(a)]. The corresponding q vectors for intra-valley and inter-valley scattering have values, respectively, near the Γ and K points. We found that many dispersive Raman spectra that have been observed experimentally, but never assigned

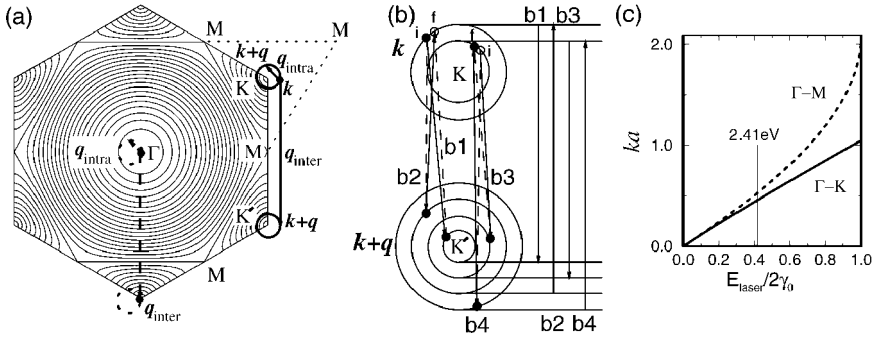

FIGURE 2 (a) Energy contours of 2D graphite. $E = E(k)$, and $E(k+q)$ are shown as thick solid circles around the K or K′ points in the Brillouin zone of 2D graphite. When the energy increases, the circles are deformed to a triangle, denoted by dotted lines which connect three nearest neighbor M points to a K point. Dotted circles around the K and Γ points give all possible intra-valley q_{intra} and also inter-valley q_{inter} phonon wave vectors measured from Γ, for a given k vector shown near the upper-right K point. (b) (left) Inter-valley, double resonance scattering. "i" and "f" denote the initial and final electron k states, respectively. The b1, b2, b3, and b4 correspond to the four scattering processes of Figure 1(b). Solid and open dots denote the resonant and non-resonant energy positions. Electronic transitions for electrons with momentum k occur on two solid circles around the K point, and the electron is then scattered to the four solid circles around the K′ point. (right) The vectors b1, b2, b3, and b4 denote the $q = 2k$ vectors which give the D-band phonon frequency. (c) The trigonal warping effect. The distance of k from the K point is plotted as a function of E_{laser}, normalized by the lattice constant a and the tight-binding parameter $2\gamma_0$ which are used to obtain dimensionless quantities for making the plot. The two lines denote the energy dispersions along Γ−M and Γ−K, which give the most and the least distant k vectors. In the figure we show the distribution of k that can be probed for $E_{\text{laser}} = 2.41$ eV.

previously, can now be assigned to specific features in the phonon energy dispersion of graphite by double resonance theory [6]. Thus double resonance Raman measurements can be used for determining the phonon energy dispersion relations, when combined with theory. In solid state physics, phonon dispersion relations are normally determined by inelastic neutron scattering, which requires large single crystals. Such crystals are not easily obtained in nano-materials or disordered materials. Moreover, the conventional methods of inelastic neutron scattering or electron energy loss spectroscopy do not have high accuracy in energy resolution near the BZ boundary. Double resonance Raman spectra, however, provide an alternative experimental method which is suitable for measurements on disordered and nano-scale materials and for observing the phonon frequency at the zone boundary.

In this paper, we discuss the spectral shape and linewidth of the D-band. Here we show that the four different processes associated with double resonance Raman scattering give two distinct D-band phonon frequencies. However, the trigonal warping effect in which the energy contours deform from a circle to a triangle with increasing energy around the K point (corner of the hexagonal BZ) will smear the double resonance Raman peaks. We evaluate these effects quantitatively for graphite. Next we consider the double resonance condition for isolated single wall carbon nanotubes.

DOUBLE RESONANCE PROCESSES OF GRAPHITE

In Figure 2(b) we show the four inequivalent double resonance processes occurring in second-order, *inter-valley* scattering. Two processes (b1 and b2) are for resonance with the incident photon and the other two (b3 and b4) are for resonance with the scattered photon. The notation from b1 to b4 is the same as for Figure 1(b). Here for simplicity, we show one scattering process from K to K′ for the b1 to b4 processes. In Figure 2, solid and open dots denote the resonant and non-resonant energy positions, and "i" and "f" denote initial and final states, respectively. In Figure 2(b), the final k states ("f") are slightly shifted from the initial k states ("i") in order to show the process clearly. The large and small circles around K are energy contours for $E(k) = E_{\text{laser}}/2$ and $E(k) = [E_{\text{laser}} - \hbar\omega(q)]/2$, respectively, on which k vector can be selected. Here we assume that $E(k)$ is symmetric in energy around the Fermi energy. Four circles around K′ are energy contours for $E(k+q) = [E_{\text{laser}} + \hbar\omega(q)]/2$, $(E_{\text{laser}}/2)$, $[E_{\text{laser}} - \hbar\omega(q)]/2$, and $(E_{\text{laser}}/2) - \hbar\omega(q)$ from the largest to the smallest, and these contours correspond to $k+q$ vectors for the b4, b2, b3 and b1 processes, respectively. In the 2D BZ, the difference in diameter of the energy contour circles is much smaller than the KK′ distance. Here the difference in diameter is artificially enlarged in Fig. 2(b) for understanding the processes.

When we consider an initial k point, the possible $k+q$ vectors are on the circles denoting the energy contour. This means that for q vectors measured from the Γ (center) point in the BZ, the end of the q vector is a circle which touches (or almost touches) the K point [see dotted circles of q_{inter} in Fig. 2(a)] for the b2 and b3 (or for the b1 and b4) processes. Since the phonon dispersion is nearly symmetric around the K point, the same distance of the end point of the q vector from the K point (hereafter we measure the distance of the end of the wave vectors from the K point, and we simply call this the distance of the q vector) gives the same phonon frequency. The distances of the q vectors on a circle have singularities at the distances $q = 0$ and $q = 2k$, where k is the radius of the circle. When

we rotate the initial k along the circle of the energy contour of the K point as shown by the dotted circle in Figure 2(a), the circles of the q vector also rotate around the K point, while touching the K point. Thus all q with $q \leq 2k$ can be satisfied by the double resonant condition. However, the singularities in the density of q vectors at $q = 0$ and at $q = 2k$ give peaks for the D-band feature in the calculation. The $q = 0$ peak could give the K point phonon frequency ($1250\,\mathrm{cm}^{-1}$), and this peak does not show any dispersive nature by changing E_{laser}, and this process is observed as a weak peak around $1250\,\mathrm{cm}^{-1}$ in the experiment. A possible explanation why the $q = 0$ Raman peak is weak in the experiment is that the electronic eigenfunctions for k and $k + K$ (K is the vector of ΓK) do not couple to each other by an impurity, while the k and $-k$ states couple to each other in the presence of a single defect. A calculation of the scattering matrix elements for an electron by possible defects is needed to account for the discrepancy between theory and experiment relative to the $q = 0$ peak, which will be a problem in the future. Hereafter we consider only $q = 2k$ phonons. In the right part of Figure 2(b) we show $q = 2k$ phonon wave vectors for four different processes. Since the $q = 2k$ vectors for b1 and b3 and for b2 and b4 have the same length, there exists two q vectors, each with different lengths. If all four processes have similar scattering matrix elements, and if there are no other effects, we could expect two peaks in the D-band spectra for a given laser energy. The higher D-band peak comes from the processes for which the elastic scattering comes first in the two consecutive scattering processes, while the lower D-band peak comes from those where inelastic scattering comes first. It is stressed that the two D-band peaks does *not* come from resonances with incident and scattered photons.

However, we do not observe two distinct peaks in the D-band spectra in the experiment, and this may relate to several factors which determine the line width of the D-band. Here we estimate the distribution of q vectors which contribute to the linewidth. An important factor is the trigonal warping effect, by which the energy contour is modified from a circle to eventually become a triangle [Fig. 2(a)]. Thus the difference between the q vectors discussed above should be compared with the distribution of k vectors due to the trigonal warping effect. For this estimate we simply use a linear approximation for the symmetric energy dispersion, $E(k) = \pm\sqrt{3}\gamma_0 ka/2$ in which $\gamma_0 = 2.90\,\mathrm{eV}$ and $a = 0.246\,\mathrm{nm}$ are, respectively, the tight binding overlap energy parameter and the lattice constant. The difference between the initial k vectors for the b1 and b3 processes corresponds to the phonon energy of the D-band, $0.167\,\mathrm{eV}$, $\Delta(ka) = 0.167/\sqrt{3}\gamma_0 = 0.033$. Thus, the difference between the two D-band peaks is twice this value, $\Delta(ka) = 0.066$. On the other hand, from the trigonal warping effect for $E_{\mathrm{laser}} = 2.41\,\mathrm{eV}$, we estimate $\Delta(ka) = 0.069$

using the tight-binding electron dispersion [8]. In Figure 2(c), we show the distance of k from the K point as a function of E_{laser} normalized by the lattice constant a and tight-binding parameter $2\gamma_0$. The two lines denote the energy dispersion in the directions of $\Gamma-$M and $\Gamma-$K, which give the most and the least distant k vectors, respectively. For a given $E_{\text{laser}} = 2.41$ eV, the difference between the k gives $\Delta(ka) = 0.069$, which is relevant to the linewidth of the spectra. Thus, the separations of the two peaks and the width for each peak resulting from the trigonal warping effect are almost of the same order, and for this reason we can fit the two peaks to a single broadened feature in the experimental spectrum. When E_{laser} increases, the trigonal warping effect quickly increases, and thus the broadening of the D-band [9] becomes significant, so that the contribution from the incident and scattered peaks should hardly be resolved. The corresponding intensity becomes weak with increasing E_{laser}, which is consistent with the experimental data, in which the intensity of the D-band decreases as E_{laser} increases [9].

The situation will be different for the overtone G′-band mode since the energy difference between the incident and scattered electron energy becomes twice as large. However, there are no b2 or b3 processes in the second-order, *two-phonon* processes, but rather there is only one q vector in the G′-band which comes from the b1 and b4 processes. It is noted here that both the k and $k+q$ states of the b4 process for the G′-band exist on circles having a smaller diameter that those for the D-band. This is the reason why the G′-band gives such a strong intensity with such a narrow width relative to that of the D-band, in addition to the fact that no defect states are needed for observing the G′-band. In this sense, though the G′ band is an overtone mode of the D-band, the scattering process is much different.

An another important factor is the three dimensional (3D) electron dispersion relations of graphite. In 3D graphite, there is an energy dispersion along the KH axis of the BZ in the direction perpendicular to the 2D graphite plane, and this dispersion is described by the Slonczewski and Weiss (SW) tight-binding parameter $\gamma_1 = 0.39$ eV [10] describing the interlayer interaction, which corresponds to an ambiguity of $\Delta(ka) = 2 \times \gamma_1/\sqrt{3}\gamma_0 = 0.15$. If this value is adopted, the differences between the q vectors for the different processes cannot be seen. However, this $\Delta(ka)$ value is overestimated, since the density of k states is not homogeneous in the direction of KH. Moreover, in disordered graphite, the layer stacking is not well ordered, and the material with an uncorrelated layer stacking (called turbostratic graphite), has an interlayer separation larger (3.44 Å) than that of single crystal of graphite (3.35 Å). Thus this ambiguity in $\Delta(ka)$ for disordered 2D graphite (and for single wall nanotubes) may be considered as a minor effect compared to the trigonal

warping effect. It should be mentioned that in 3D graphite, two G′ band peaks are observed. This is because of the two different energy dispersions along KH described by the γ_1 and γ_2 interlayer SW parameters [10]. Thus the G′-band Raman spectra clearly distinguish 2D from 3D graphite [11].

The overall peak intensity and linewidth of the D-band spectra should reflect all these features and effects. Also the phonon dispersion for optical phonon dispersion as a function of q is not so steep as for the acoustic phonons. In fact, the qa value for KM is $2\pi/3 = 2.09$ which is much larger than the above $\Delta(qa)$, and the slope of the optical phonon frequency associated with the D-band in the middle of KM is $275\,\mathrm{cm}^{-1}$ per $qa = 1$. Thus $\Delta(qa) = 0.066$ gives $18\,\mathrm{cm}^{-1}$ which corresponds to the separation of the two peaks of the D-band. This value is smaller than the observed linewidth of the D-band by about $50\,\mathrm{cm}^{-1}$. However, Tan *et al.* [12] and Cancado *et al.* [13] have observed that the Stokes and anti-Stokes spectra of disordered graphite at several laser energies have different phonon frequencies from one another (by about $7\,\mathrm{cm}^{-1}$) [12,13]. When we put the D-band phonon energy of 0.137 eV into the dispersion formula of the D-band spectra, $53\,\mathrm{cm}^{-1}/\,\mathrm{eV}$, we get $7\,\mathrm{cm}^{-1}$, which is consistent with the dispersive energy. Here it is noted that the center of mass of the two peaks is shifted by 0.137 eV ($9\,\mathrm{cm}^{-1}$). This is because the four different processes of the anti-Stokes spectra can be considered to be related by time reversal symmetry to the corresponding Stokes processes by changing E_{laser} to $E_{\mathrm{laser}} + \hbar\omega_{\mathrm{ph}}$. Thus we conclude that the energy shift between the Stokes and anti-Stokes D-band peaks is half of the separation between the two peaks.

DOUBLE RESONANCE PROCESSES OF NANOTUBES

The double resonance Raman theory of graphite can apply to the D-band of SWNTs. In the case of SWNTs, the 2D electronic energy bands of graphite are zone-folded along the circumferential direction, which is realized by cutting the 2D BZ by lines, to obtain a set of 1D energy dispersion relations for SWNTs. For the 1D energy dispersion relations, the joint density of states (JDOS) is singular at the energy band edge, and this is known as a van Hove singularity (VHS). Resonant Raman measurements of an isolated single wall carbon nanotube are possible [14] when an optical transition occurs between VHSs from the valence to the conduction bands. In SWNT bundles we observe a similar dependence of ω_D on E_{laser} to that of graphite, but with a superimposed oscillatory behavior [15], which can be explained by the double resonance process [5,16,17]. In the double resonance theory for SWNTs, the cross section of the energy contours and the cutting lines of the 1D BZ are the k points k_{ii} that satisfy the double resonance condition. When the energy contour *touches* the cutting line, the touching point

corresponds to a VHS singular k point for a given (n, m) chirality. The distance of this k_{ii} point from the K point of the BZ determines the resonant energy E_{ii} and the phonon frequency ω_D. Since the direction of the cutting lines depend on chiral angle [8], the chirality dependence of ω_D for isolated SWNTs is well explained by the distance of the k_{ii} from the K point [17]. The trigonal warping effect also gives a splitting of the electronic density of states for metallic nanotubes, and this splitting gives two resonant conditions for a SWNT. This trigonal warping effect has recently been observed experimentally in the G′-band spectra of isolated SWNTs [16].

For (n, m) nanotubes, the K point is folded into the 1D BZ at the Y point, and the distance of the Y point from the center of the 1D BZ, Γ, is given by [8], $\Gamma Y = (m/d_R|\mathbf{K}_2|$, where d_R is the greatest common divisor (gcd) of $(2m + n)$ and $(2n + m)$, and $|\mathbf{K}_2|$ is the length of the one-dimensional BZ. After some calculation, it can be shown that for all semiconducting nanotubes and all metallic nanotubes with $d_R = d$, the Y point becomes a Γ point ($\Gamma Y = 0$), and that the remaining type of metallic nanotube for which $d_R = 3d$, the Y point is at a one third position of the 1D BZ line ($\Gamma Y = \pm|K_2|/3$) [8]. In particular, all zigzag nanotubes are of the $d_R = d$ type, while all armchair nanotubes are of the $d_R = 3d$ type. For general chiral metallic nanotubes, the type of metallic nanotube depends on (n, m). The second-order, one-phonon, inter-valley and double resonance condition is satisfied in the both cases. This is consistent with the recent experiments that the D-band is observed in semiconducting nanotubes. The linewidth of D-band becomes much smaller ($10\,\mathrm{cm}^{-1}$) for SWNTs, since the condition for double resonance is limited only to k_{ii} points, and thus all four processes may not occur at the same time. Thus, all four processes might not occur equally in the case of SWNTs. However, some SWNTs show relatively large D-band line widths (up to $20\,\mathrm{cm}^{-1}$), which are chirality dependent. The origin of the distribution of line widths may come from the double resonance conditions for more than two electron energy dispersions occurring for the k_{ii} points for a given SWNT. Detailed results on this topic will be reported in the near future.

CONCLUSIONS

In summary, the Stokes D-band spectra of graphite and SWNTs are explained by second-order, one-phonon emission, and inter-valley, double resonant scattering processes. There are four different double resonant scattering processes, which give two inequivalent D-band peaks and one G′ peak. The trigonal warping effect will give a large distribution of initial k vectors and thus a broadening larger than the separation between the two peaks is expected. The double resonance theory of SWNTs gives a chirality

dependent D-band phonon frequency which is relevant to the van Hove singular k_{ii} points, and which restricts the occurrence of some of the four double resonance processes.

REFERENCES

[1] Tuinstra, F. & Koenig, J. L. (1970). *J. Chem. Phys.*, *53*, 1126.
[2] Dresselhaus, M. S. & Eklund, P. C. (2000). *Advances in Physics*, *49*, 705–814.
[3] Dresselhaus, M. S., Dresselhaus, G., Jorio, A., Souza Filho, A. G., & Saito, R. (2002). *Carbon*, in press.
[4] Thomsen, C. & Reich, S. (2000). *Phys. Rev. Lett.*, *85*, 5214.
[5] Kürti, J., Zólyomi, V., Grüeneis, A., & Kuzmany, H. unpublished.
[6] Saito, R., Jorio, A., Souza Filho, A. G., Dresselhaus, G., Dresselhaus, M. S., & Pimenta, M. A. (2002). *Phys. Rev. Lett.*, in press.
[7] Martin, R. M. & Falicov, L. M. (1975). In: *Light-Scattering in Solids*, Cardona, M. (Ed.), Springer-Verlag: Berlin.
[8] Saito, R., Dresselhaus, G., & Dresselhaus, M. S. (1998). *Physical Properties of Carbon Nanotubes*, Imperial College Press: London.
[9] Pócsik, I., Hundhausen, M., Koós, M., & Ley, L. (1998). *J. Non-Cryst. Solids*, *1083*, 227–230.
[10] Slonczewski, J. C. & Weiss, P. R. (1957). *Phys. Rev.*, *109*, 272.
[11] Wilhelm, H., Lelaurian, M., McRae, E., & Humbert, B. (1998). *J. Appl. Phys.*, *84*, 6552.
[12] Tan, P. H., Deng, Y. M., & Zhao, Q. (1998). *Phys. Rev. B*, *58*, 5435.
[13] Cancado, L. G., Pimenta, M. A., Saito, R., Jorio, A., Souza Filho, A. G., Dresselhaus, G., & Dresselhaus, M. S. unpublished.
[14] Jorio, A., Saito, R., Hafner, J. H., Lieber, C. M., Hunter, M., McClure, T., Dresselhaus, G., & Dresselhaus, M. S. (2001). *Phys. Rev. Lett.*, *86*, 1118–1121.
[15] Pimenta, M. A., Hanlon, E. B., Marucci, A., Corio, P., Brown, S. D. M., Empedocles, S. A., Bawendi, M. G., Dresselhaus, G., & Dresselhaus, M. S. (2000). *Brazilian J. Phys.*, *30*, 423–427.
[16] Souza Filho, A. G., Jorio, A., Dresselhaus, G., Dresselhaus, M. S., Swan, A. K., Goldberg, B. B., Ünlü, M. S., Saito, R., Hafner, J. H., Lieber, C. M., & Pimenta, M. A. unpublished.
[17] Souza Filho, A. G., Jorio, A., Dresselhaus, G., Dresselhaus, M. S., Saito, R., Swan, A. K., Ünlü, M. S., Goldberg, B. B., Hafner, J. H., Lieber, C. M., & Pimenta, M. A. (2001). *Phys. Rev. B*, *64*, in press.